



# Protein restriction cycles reduce IGF-1 and phosphorylated Tau, and improve behavioral performance in an Alzheimer's disease mouse model

Edoardo Parrella,<sup>1</sup> Tom Maxim,<sup>1</sup> Francesca Maialetti,<sup>2</sup> Lu Zhang,<sup>1</sup> Junxiang Wan,<sup>1</sup> Min Wei,<sup>1</sup> Pinchas Cohen,<sup>1</sup> Luigi Fontana<sup>3,4,5</sup> and Valter D. Longo<sup>1</sup>

<sup>1</sup>Longevity Institute, Davis School of Gerontology, and Department of Biological Sciences, University of Southern California, Los Angeles, CA, USA

<sup>2</sup>Division of Nutrition and Aging, Istituto Superiore di Sanità, Rome, Italy

<sup>3</sup>Division of Geriatrics and Nutritional Science, Washington University in St. Louis St. Louis, MO, USA

<sup>4</sup>Department of Medicine, Salerno University School of Medicine, Salerno, Italy

<sup>5</sup>Healthy Aging Platform, CEINGE Biotechnologie Avanzate, Napoli, Italy

## Summary

**In laboratory animals, calorie restriction (CR) protects against aging, oxidative stress, and neurodegenerative pathologies. Reduced levels of growth hormone and IGF-1, which mediate some of the protective effects of CR, can also extend longevity and/or protect against age-related diseases in rodents and humans. However, severely restricted diets are difficult to maintain and are associated with chronically low weight and other major side effects. Here we show that 4 months of periodic protein restriction cycles (PRCs) with supplementation of non-essential amino acids in mice already displaying significant cognitive impairment and Alzheimer's disease (AD)-like pathology reduced circulating IGF-1 levels by 30–70% and caused an 8-fold increase in IGFBP-1. Whereas PRCs did not affect the levels of  $\beta$  amyloid ( $A\beta$ ), they decreased tau phosphorylation in the hippocampus and alleviated the age-dependent impairment in cognitive performance. These results indicate that periodic protein restriction cycles without CR can promote changes in circulating growth factors and tau phosphorylation associated with protection against age-related neuropathologies.**

**Key words:** aging; alzheimer; IGF-1; IGFBP-1; protein restriction; tau.

## Introduction

Calorie restriction (CR) without malnutrition is effective in protecting the brain against aging and oxidative stress (Martin *et al.*, 2006). Several studies support a beneficial role for this dietary intervention in protecting against age-dependent decay in cognitive performance in rodents (Fontan-Lozano *et al.*, 2008). In addition, CR shows remarkable neuroprotective properties against neurodegenerative

diseases including stroke, Parkinson's disease (PD), Huntington's disease (HD), and Alzheimer's disease (AD) in several animal models (Mattson, 2005; Patel *et al.*, 2005).

Recent studies in different AD mouse models reported that reducing food intake can diminish AD-related neuropathologies and cognitive dysfunction. For example, CR reduces the progression of  $\beta$  amyloid ( $A\beta$ ) deposition in the hippocampus and cerebral cortex of mice carrying familial Alzheimer's disease mutations in the amyloid precursor protein (APP) and/or presenilin 1 (Patel *et al.*, 2005; Wang *et al.*, 2005; Mouton *et al.*, 2009). CR ameliorates neurodegenerative phenotypes assessed by object recognition and contextual fear conditioning tests and reduces tau hyperphosphorylation in cDKO (conditional double knockout) AD mice (Wu *et al.*, 2008). Mattson and coworkers have shown that CR can also ameliorate age-related memory impairment and decrease  $A\beta$  and phosphorylated tau accumulation in a triple transgenic mouse (3xTg-AD) model that overexpresses mutated human genes linked to AD (PS-1, APP) and frontotemporal dementia (tau) (Halagappa *et al.*, 2007). Furthermore, studies in human populations suggest that diet plays an important role in AD and reduced food intake may protect against this pathology. For example, an epidemiological study by Luchsinger and colleagues indicates that individuals with a low-calorie intake may have a reduced risk of developing AD (Luchsinger *et al.*, 2002).

Among the large number of metabolic and physiological changes caused by CR, the reduction in growth hormone (GH)/insulin-like factor (IGF-1) signaling may be important for its protective effects (Fontana *et al.*, 2010). Circulating IGF-1 is a hormone produced primarily by the liver that regulates energy metabolism, cell proliferation, cell differentiation, body size, and lifespan. IGF-1 levels are regulated by calorie and/or protein availability. Long-term CR decreases serum IGF-1 concentration by approximately 30–40% in rodents (Thissen *et al.*, 1994) but not in humans unless protein intake is also reduced (Fontana *et al.*, 2008). Mutations that decrease the activity of growth hormone (GH)/IGF-1 signaling, similarly to CR, can extend longevity and enhance stress resistance in a wide range of organisms and systems (Kenyon, 2005), including the mammalian central nervous system (CNS) (Parrella & Longo, 2010). Although the overlap between the pathways altered by these nutritional and genetic interventions seems to be only partial, it has been proposed that decline in IGF-1 levels can mediate part of the beneficial effects caused by CR (Sonntag *et al.*, 1999; Longo & Finch 2003). In support of this theory, it has been shown recently that reducing IGF-1 signaling in an AD mouse carrying APP and PS-1 mutations protects against Alzheimer's-like disease symptoms including cognitive deficits and neuroinflammation (Cohen *et al.*, 2009). Notably, GH receptor-deficient (GHRD) mice and humans are protected from major diseases (Ikeno *et al.*, 2009; Masternak *et al.*,

## Correspondence

Valter D. Longo, Longevity Institute, Davis School of Gerontology, University of Southern California, 3715 McClintock Avenue, Los Angeles, CA 90089-0191, USA. Tel.: +1 213 7406212; fax: +1 213 8215714; e-mail: vlongo@usc.edu

Accepted for publication 10 January 2013

2009; Guevara-Aguirre *et al.*, 2011); and GHRD mice live 40% longer (Coschigano *et al.*, 2000). Moreover, a study of a cohort of Ashkenazi Jewish centenarians identified genetic alterations in human IGF-1 receptor (IGF-1R) that result in reduced IGF-1 signaling among the centenarians compared with controls (Suh *et al.*, 2008). On the other hand, the effect of IGF-1 or IGF-1R deficiency on lifespan is inconsistent (Bokov *et al.*, 2011), suggesting that reduced IGF-1 may be only one of the mediators of the anti-aging effects of GHR deficiency and that insulin and other factors may also play a key role.

Protein and amino acid (AA) availability is fundamental in regulating IGF-1 gene expression. Protein restriction not only decreases IGF-1 production rate but also accelerates its clearance, regulates IGF-1 interaction with IGF binding proteins (IGFBPs), and attenuates IGF-1 biological actions (Ketelslegers *et al.*, 1995). Since long-term CR is very difficult to maintain and is unavoidably associated with weight loss, loss of sex drive, hunger, feeling cold at normal room temperature, and possible immune system side effects, we investigated whether a long-term alternation of cycles of a normal and a protein restricted diet (protein restriction cycles, PRCs) could reduce GHR/IGF-1 levels/signaling and ameliorate the AD-like symptoms in 3xTg-AD mice that accumulates both the A $\beta$  and tau pathologies associated with AD.

## Results

### PRC regimen does not cause a chronic low body weight state nor an overall decrease in calorie intake

After 7-day on the PR diet, both 3xTg-AD and WT mice lost between 13 and 17% of the initial body weight, which was fully recovered during the following 7 days of refeeding with the normal diet (Fig. 1B, repeated measures ANOVA followed by Newman–Keuls test:  $P < 0.001$ , control regimens compared with PRC regimens). A similar body weight profile was maintained by mice subjected to PRC regimen during the whole 18 weeks of dietary treatment (Fig. 1C). However, we noticed a significant difference between WT and 3xTg-AD groups, with 3xTg-AD rodents gradually and slightly losing weight at week 6–7 (Fig. 1C, repeated measures ANOVA followed by Newman–Keuls test:  $P < 0.05$ , 3xTg-AD control vs. WT control and 3xTg-AD PRC vs. WT PRC). Considering the gradual body weight drop in the 3xTg-AD control group, the age-dependent weight loss of 3xTg-AD PRC mice on the protein restricted (PR) diet appears to be mostly dependent on the mutations and not the diet. Taken together, these data indicate that PRCs were not associated with a chronic underweight state in both WT and 3xTg-AD mice, although longer periods of refeeding with the normal diet may be required to allow weight maintenance after long-term cycles of protein restriction.

Next, to investigate a possible impact of the total calorie intake during the diet regimen, we monitored the food consumption at the beginning (weeks 1 and 2) and the end (weeks 17 and 18) of the dietary intervention. At the beginning of the treatment (weeks 1 and 2), during the initial 7 days of PR diet (days 1–7), average calorie intake was reduced by 24.3% in WT and 24.2% in 3xTg-AD mice

(SFig. 1A, *t*-test:  $F = 2.46$  and  $3.79$ , respectively,  $P < 0.001$ ). Diet lacking essential AA presents low palatability and most animals, including rodents, reduce their food intake after ingesting food lacking essential AA (Gietzen *et al.*, 2007). However, during the refeeding (days 8–14 of the PR cycle) average caloric intake was increased by 22.5% in WT and 17.2% in 3xTg-AD mice (SFig. 1A, *t*-test:  $F = 1.53$  and  $P < 0.01$  for WT,  $F = 1.62$  and  $P < 0.05$  for 3xTg-AD). A similar caloric intake profile was observed at the end of the dietary intervention (weeks 17 and 18). Average caloric intake was decreased by 20.3% in WT and 10.5% in 3xTg-AD mice during the PR diet feeding (SFig. 1B, *t*-test:  $F = 3.57$  and  $P < 0.05$  for WT,  $F = 27.78$  and  $P > 0.05$  for 3xTg-AD). Again, the normal diet refeeding period was coupled to a significant increase of caloric consumption (SFig. 1B, 40.1% in WT and 25.3% in 3xTg-AD *t*-test:  $F = 3.47$  and  $P < 0.001$  for WT,  $F = 1.50$  and  $P < 0.05$  for 3xTg-AD).

The average caloric intake calculated by combining the values for the periods of both PR and normal diet refeeding was similar to that of the standard diet-fed control group for both the first and the final weeks of the treatment (Fig. 1D and 1E, *t*-test,  $P > 0.05$ ). We concluded that the PRC regimen was associated with a modest but unavoidable CR only during the PR diet phase (albeit with diminishing effect over the long term), ranging between 19 and 17% for WT and 25.6 and 13% for 3xTg-AD, which is counterbalanced by an increase of calories intake during the following normal diet refeeding period. This caloric intake profile of PRC intervention was different not only from a CR regimen but also from intermittent fasting (IR) (or every other day feeding – EODF), another dietary restriction consisting in food deprivation for 24 h every other day and characterized by a 20–30% caloric intake reduction over time with beneficial effects similar to CR (Martin *et al.*, 2006).

### PRC regimen does not cause a significant reduction of blood glucose levels

Blood glucose levels undergo remarkable changes during food restriction. For example, prolonged 20–40% CR in rodents can cause blood glucose reduction between 20 and 40% (Lee & Longo, 2011). PRC regimen, however, did not promote a significant change in blood glucose levels, but caused a trend of reduction in glucose concentration (17% in WT and 8% in 3xTg-AD mice) only at the end of the PR diet-feeding period (Fig. 2A). These data support our conclusion that the effects of PRCs are not due to CR.

### PRC regimen reduces circulating IGF-1 levels by 30–70%, IGFBP-3 by 20–40%, and increase IGFBP-1 by 3–8 folds in 3xTg-AD mice

Approximately 95% of the IGF-1 that acts on the brain has been shown to be derived from the liver (Yamamoto & Murphy, 1995). Although IGF-1, its receptor and binding proteins are also present and locally produced in the brain, IGF-1 is actively transported across the blood–brain barrier, and therefore changes in circulating IGF-1 can lead to changes in IGF-1 input to the brain (Carro *et al.*, 2000). The bioavailability and bioactivity of IGF-1 is regulated by

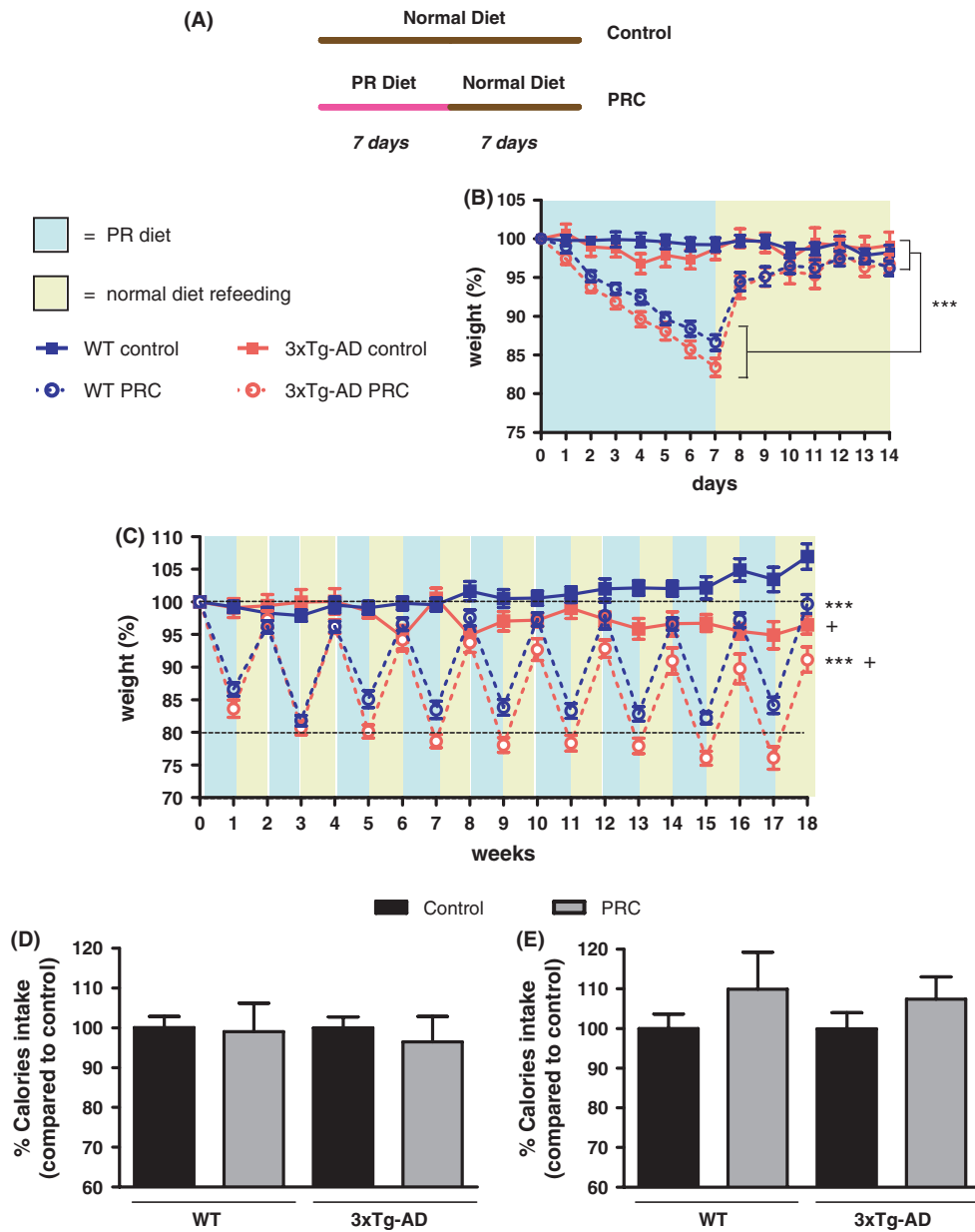


**Fig. 1** Body weight and calories intake profiles. (A) Diagram showing the Control and PRC dietary regimens used in the study. (B, C) Mouse body weights were measured and plotted as percentage of the initial weight scored at day zero (13–15 animals per group). The mice were weighed daily the first 2 weeks (B) and weekly for the remaining 16 weeks (C). (B) During the first 2 weeks of dietary intervention WT and 3xTg-AD mice subjected to PRC regimen showed a significantly different body weight profile when compared with corresponding controls ( $***P < 0.001$ ). (C) The different body weight profile between WT and 3xTg-AD PRC groups and corresponding controls was maintained over the whole 18 weeks of dietary treatment ( $***P < 0.001$ ). Moreover, we found a significant difference between body weight profiles of 3xTg-AD control and PRC groups and corresponding WT animals ( $+P < 0.05$ , 3xTg-AD control vs. WT control and 3xTg-AD PRC vs. WT PRC). (D, E) Calories intake normalized for grams of body weight was scored daily at the beginning (weeks 1 and 2, D) and at the end of the dietary treatment (weeks 17–18, E) and was expressed as percentage calculated for the combined 2 weeks of PR diet and normal diet refeeding.

IGF-binding proteins (IGFBPs), a family of six proteins acting as carriers for IGFs (Jones & Clemmons, 1995). Among the different binding proteins, IGFBP-3 and IGFBP-1 play a prominent role in IGF-1 bioavailability.

IGFBP-3 is quantitatively the most abundant IGFBP, binding more than 80% of the circulating IGF-1 and protecting it from rapid degradation or clearance from the serum (Jones & Clemmons, 1995).

Differently from the other IGFBPs, IGFBP-1 inhibits IGF-1 action by binding to IGF-1 itself and preventing its binding to IGF receptors (Jones & Clemmons, 1995).

IGF-1 measurement revealed that 3xTg-AD had higher circulating levels of the hormone compared with WT (Fig. 2B, *t*-test: WT vs. 3xTg-AD,  $P < 0.01$ ). In 3xTg-AD mice, IGF-1 levels were reduced by PRC regimen not only during the PR diet period (Fig. 2B, 70% reduction, 3xTg-AD control vs. 3xTg-AD PRC at the end of PR diet

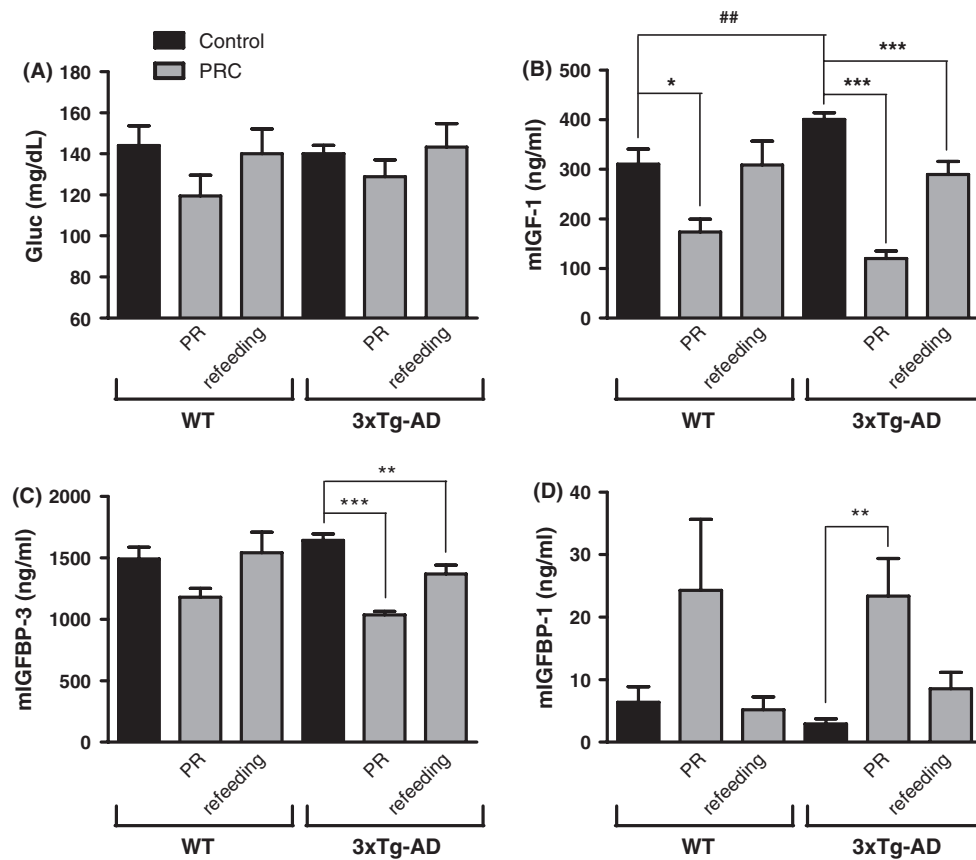


**Fig. 2** PRC regimen does not modify blood glucose levels but modulate circulating IGF-1 and IGFBPs. (A) Blood glucose levels are expressed as concentration ( $\text{mg dL}^{-1}$ ). No significant difference was detected between the experimental groups (6–13 samples per group). (B–D) Mouse Serum IGF-1 and IGFBP-1/3 levels are expressed as concentration ( $\text{ng mL}^{-1}$ ) (3–7 samples per group). (B) WT mice sacrificed at the end of PR diet cycle displayed significantly lower IGF-1 levels when compared with corresponding control group ( $*P < 0.05$ ). 3xTg-AD mice showed a significant reduction in IGF-1 levels not only during the PR diet cycle but also during the normal diet refeeding ( $***P < 0.001$ ). We detect a significant difference between WT control and 3xTg-AD control groups ( $##P < 0.01$ ). (C) 3xTg-AD mice showed a significant reduction in IGFBP-3 levels not only when fed with the PR diet ( $***P < 0.001$ ) but also during the refeeding cycle ( $**P < 0.01$ ). (D) We determined a significant increase in IGFBP-1 levels at the end of the PR cycle in 3xTg-AD mice ( $**P < 0.01$ ).

cycle, One-Way ANOVA  $P < 0.001$ ) but also during the normal diet refeeding (Fig. 2B, 28% reduction, 3xTg-AD control vs. 3xTg-AD PRCs at the end of normal diet refeeding cycle, One-Way ANOVA  $P < 0.001$ ). A similar but weaker effect was detected in WT mice at the end of PR diet (Fig. 2B, 44% reduction, WT control vs. WT PRC at the end of PRCs diet, One-Way ANOVA  $P < 0.05$ ). Circulating levels of IGFBP-3 were significantly decreased by the PRC regimen at the end of both PR diet and refeeding periods in 3xTg-AD mice (Fig. 2C, 37% reduction, 3xTg-AD control vs. 3xTg-AD PRC at the end of PR cycle, One-Way ANOVA  $P < 0.001$ ; 17% reduction, 3xTg-AD control vs. 3xTg-AD PRC at the end of normal diet refeeding, One-Way ANOVA  $P < 0.01$ ). In WT mice, although we noticed a trend for a reduction during PR diet feeding, PRCs failed to cause significant changes in IGFBP-3 levels. Finally, in 3xTg-AD mice, PRCs promoted a major increase in circulating IGFBP-1 levels at the end of PR period (Fig. 2D, 8-fold increase, 3xTg-AD control vs. 3xTg-AD at the end of PR cycle,  $P < 0.01$  One-Way ANOVA). Albeit we observed a trend for an increase of IGFBP-1 during PR, PRC regimen did not cause a significant modulation of its serum levels in WT mice (Fig. 2D).

Taken together, these results clearly indicate that 18–19 weeks of PRC regimen promoted a strong modulation of IGF-1 and IGFBPs

whose combined effect was a reduction of circulating levels of IGF-1. The effect was greater in 3xTg-AD mice.

### PRC regimen alleviates age-dependent working memory deficits in 3xTg-AD mice

To determine whether the PRC regimen could impact cognitive performances, we performed the Y-maze (hippocampus-dependent working memory) in both 3xTg-AD and WT mice. The mice were tested before the initiation of the dietary intervention (age 8–9 months) and once every month during the treatment. In agreement with the literature (Rosario *et al.*, 2006), 8–9-month-old 3xTg-AD male mice showed cognitive impairment detectable with Y-maze when compared with age-matched WT (Fig. 3A One-way ANOVA:  $F = 3.46$ ,  $P < 0.05$  3xTg-AD groups vs. WT control). At the age of 12.5–13.5 months, 3xTg-AD control mice exhibited a significant working memory deficit, whereas 3xTg-AD mice subjected to 18 weeks of PRC regimen did not, indicating a protective effect provided by the PRCs (Fig. 3B, One-way ANOVA:  $F = 3.46$ ,  $P < 0.05$  3xTg-AD control vs. WT control). Interestingly, after 12 weeks of treatment, the 3xTg-AD PRC mice still displayed a significant

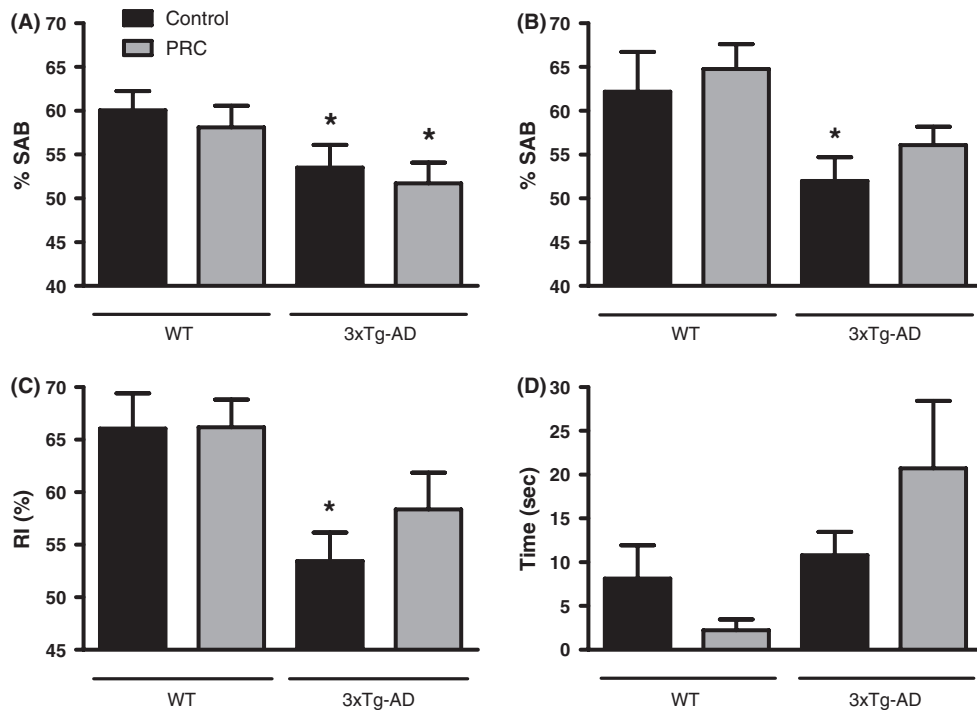


**Fig. 3** PRC regimen alleviates age-dependent behavioral changes in 3xTg-AD mice. (A and B) Shown is SAB (spontaneous alternation behavior) percentage, obtained testing the mice with the Y-maze test at 8–9 months of age, before any dietary treatment (A), or at 12.5–13.5 months of age, after 18 weeks of PRC regimen (B). (A) 3xTg-AD mice already showed working memory impairment performing significantly worse than WT control group (\* $P < 0.05$ , 13–14 mice per group). (B) Only 3xTg-AD control group performed worse than WT control (\* $P < 0.05$ , 13–14 mice per group). (C) NOR test was used to calculate RI (recognition index). RI scored for 3xTg-AD control animals was significantly lower than values calculated for WT control (\* $P < 0.05$ , 12–14 mice per group). (D) EPM test was used to score the time spent by the rodents in open arms. No significant difference was detected between the experimental groups (13–14 mice per group).

memory deficit compared with WT, suggesting that, to maximize its efficacy, the dietary intervention may have to be initiated earlier when cognitive impairment is milder (SFig. 2A, One-way ANOVA:  $F = 2.41$ ,  $P < 0.05$  3xTg-AD groups vs. WT control). We did not find significant differences in the number of arm entries among the WT and 3xTg-AD groups, suggesting that the PRCs do not interfere with the activity levels of the rodents (SFig. 3A, One-way ANOVA:  $F = 4.23$ ).

**PRC regimen alleviates short-term spatial memory deficits in 3xTg-AD mice**

Mice were tested for short-term spatial memory using the Novel Object Recognition (NOR) test. The NOR test was performed once at the end of the treatment (age 12.5–13.5 months of age). The test relies on the natural rodent tendency to preferentially explore novel objects and has been used to study working spatial memory in 3xTg-AD mice (Gulinello et al., 2009). On trial 1 of the test, the mice were allowed to explore a box containing two identical objects and the time spent exploring them was recorded. As expected, no preference for one of the two objects was detected in the different experimental groups (SFig. 3B,  $P > 0.05$ , object A vs. object B,  $t$ -test). At the end of the trial, the mice were returned to their home cages for 3 min, then placed again into the box where one of the objects was replaced with a novel one (trial 2) and the time spent exploring the objects was recorded again to calculate RI

(Recognition index) values. 3xTg-AD control mice showed a significantly lower RI compared with WT, whereas 3xTg-AD animals on the PRC regimen did not (Fig. 3C, One-way ANOVA:  $F = 2.43$ ,  $P < 0.05$  3xTg-AD control vs. WT control). These results indicate that PRCs can alleviate the spatial memory deficits caused by the 3xTg-AD mutations in mice.

**PRC regimen does not affect anxiety in the studied mice**

To function properly, the CNS requires diet-derived amino acids, including Tryptophan, Phenylalanine, Tyrosine, Histidine, Glutamine and Arginine, as substrates for the synthesis of various neurotransmitters and neuromodulators. The availability of certain amino acids can play an important role in mood regulation (Young, 1996).

To analyze the impact of the PRCs on anxiety, we tested WT and 3xTg-AD mice on the Elevated Plus Maze (EPM), a test used to analyze behavioral modifications caused by proteins undernutrition (Young, 1996). The test was performed before the treatment (age 8–9 months) and after 18 weeks of dietary intervention (age 12.5–13.5) and the time spent in the open arms scored. More time spent in the open arms reflects a lower level of anxiety.

Before the dietary intervention no significant difference was detected in the scored parameter among the experimental groups in both 3xTg-AD and WT (SFig. 2B,  $t$ -test,  $F = 1.65$ ,  $P > 0.05$  control vs. PRC). After 18 weeks of diet treatment, we noticed a reduction

in the time the mice spent in the open arms, which indicates an increased level of anxiety. The large difference between the scored parameter at the baseline and at the end of the dietary intervention is common to all the experimental groups and may be the result of the mice handling. However, we still did not detect any significant difference in the time spent in the open arms (Fig. 3D, *t*-test,  $F = 2.45$ ,  $P > 0.05$  control vs. PRC). Although we cannot rule out possible side effects on mood regulation caused by protein restriction, these results indicate that PRCs do not cause significant anxiety level changes in mice.

### PRC regimen does not reduce A $\beta$ accumulation in the 3xTg-AD mice hippocampus

To determine whether the PRC regimen could affect A $\beta$  accumulation in the brain of aged 3xTg-AD mice, brain sections were immunostained using a specific antibody against A $\beta$ . We did not find any significant difference in A $\beta$  immunoreactivity (IR) between control and PRC regimens either in the subiculum (Fig. 4A, *t*-test:  $F = 2.60$ ,  $P = 0.76$ ) or in the CA1 (Fig. 4B, *t*-test:  $F = 1.73$ ,  $P = 0.87$ ) hippocampus regions. Moreover, there was no difference in the number (Fig. 4C, *t*-test:  $F = 4.09$ ,  $P = 0.17$ ) or the size of A $\beta$  plaques between the control and PRC groups (Fig. 4D, *t*-test:  $F = 1.76$ ,  $P = 0.44$ ).

### PRC regimen reduces tau phosphorylation in the 3xTg-AD mice hippocampus

In addition to A $\beta$  accumulation, 3xTg-AD mice develop an age-dependent accumulation of phosphorylated tau that is believed to be central in the progressive cognitive impairment observed in AD. To investigate the effect of PRCs on levels of tau phosphorylation, we quantified the number of cells immunoreactive with the AT8 antibody, which recognizes the phosphorylation of tau protein at Ser 202 and 305 that is associated with AD pathology (Goedert *et al.*, 1995). We found that mice subjected to the PRC regimen showed a significant reduction in the number of phosphorylated tau positive cells compared with that in mice fed with the normal diet (Fig. 5, *t*-test:  $F = 1.31$ ,  $P < 0.05$ ). These results indicate that PRCs may inhibit tau phosphorylation either independently or downstream of A $\beta$ .

### PRC regimen does not reduce microglia activation in 3xTg-AD mice hippocampus

Next, we investigated whether the PRC regimen could affect brain inflammation. Neuroinflammation is a prominent feature of AD in agreement with a reported increase of markers of microglia activation in AD rodent models including the 3xTg-AD mice (Kitazawa *et al.*, 2005). First, we quantified the presence of activated microglia

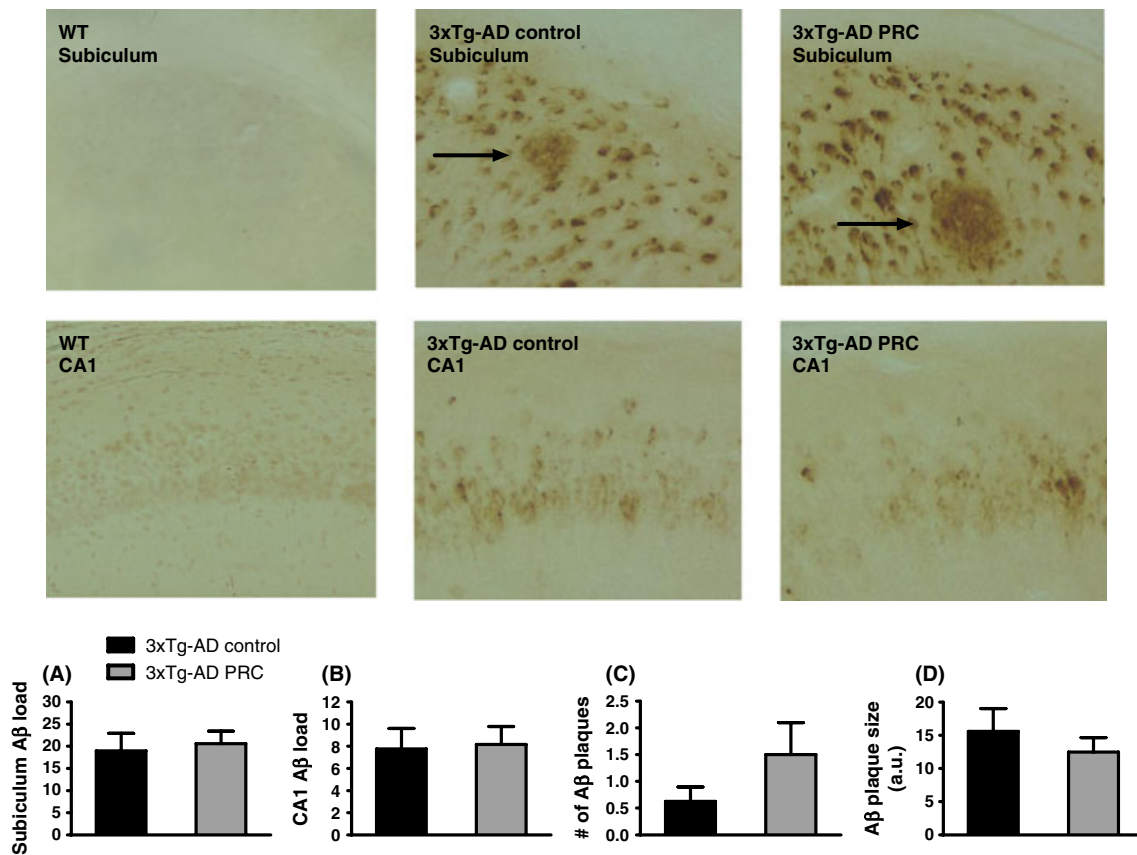


**Fig. 4** PRC regimen does not slow down A $\beta$  accumulation in 3xTg-AD mice hippocampus. Representative images showing A $\beta$  immunoreactivity in subiculum or CA1 hippocampus regions of 12.5–13.5-month-old WT control, 3xTg-AD control and 3xTg-AD PRC mice are shown. A $\beta$  plaques are indicated by arrows. Quantification of A $\beta$  accumulation by load values in subiculum and hippocampus CA1 regions is showed in (A) and (B), respectively. Number and size of A $\beta$  plaques are shown in (C) and (D). [10–12 (A, B, C) and 5–7 (D) samples per group].

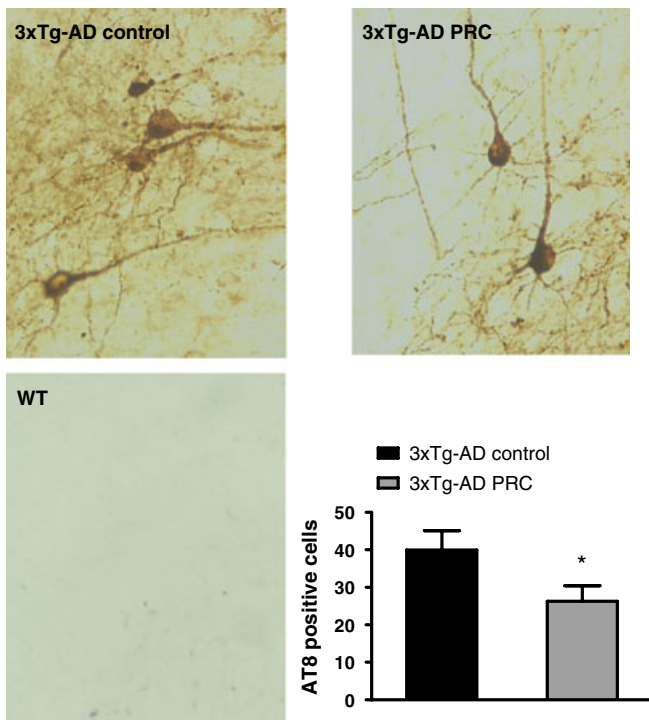


**Fig. 5** PRC regimen reduces AT8-positive neurons in 3xTg-AD mice hippocampus. Representative images showing hippocampus sections immunostained with AT8 antibody, which recognizes abnormally phosphorylated tau, of 12.5–13.5-month-old 3xTg-AD control, 3xTg-AD PRC and WT control mice are shown. Quantification of numbers of AT8-immunoreactive cells is shown (\* $P < 0.05$ , 3xTg-AD PRC vs. 3xTg-AD Control, 10–12 samples per group).

in the hippocampus using the microglia-specific marker CD11b. Our data confirmed a dramatic increase in the total number of CD11b-ir cells in the hippocampus of 3xTg-AD mice compared with WT (Fig. 6A,  $^{+++}P < 0.001$  3xTg-AD control vs. WT control). However, the total number of CD11b-ir cells in 3xTg-AD PRC mice did not differ from the value scored in 3xTg-AD mice fed the normal diet (Fig. 6A,  $P > 0.05$  3xTg-AD PRC vs. 3xTg-AD control,  $^{+++}P < 0.001$  3xTg-AD PRC vs. WT control).

Second, we quantified microglial activation based on a four-stage morphological classification ranging from resting, activated ramified, amoeboid, to phagocytic cells (Zhang *et al.*, 2011). 3xTg-AD control mice showed a prevalence of more activated stages when compared with WT (Fig. 6B: stage 1, 3xTg-AD control 20% vs. WT control 42%; stage 3, 3xTg-AD control 35% vs. WT control 22%; stage 4, 3xTg-AD control 7% vs. WT control 1%.  $^{+++}P < 0.001$  3xTg-AD control vs. WT control). Again, the PRC regimen did not influence microglia morphology in the hippocampus of 3xTg-AD mice (Fig. 6B,  $P > 0.05$  3xTg-AD PRC vs. 3xTg-AD control,  $^{+++}P < 0.001$  3xTg-AD PRC vs. WT control). These data indicate that the effect of PRCs on tau phosphorylation and behavioral defects in 3xTg-AD mice is not caused by pro-inflammatory pathways.

## Discussion

Our findings provide evidence that weekly cycles alternating a normal diet and a protein restricted diet supplemented with

nonessential amino acids regulate circulating levels of IGF-1 and IGF1BPs, reduce tau phosphorylation, and alleviate age-dependent memory deficits in a mouse model of AD.

Although PRCs could not completely reverse the cognitive decline in the 3xTg AD mouse model, the results are important in light of the fact that the PRC treatment was started when mice already showed significant cognitive impairment and AD-like pathology. 3xTgAD mice fed the normal diet displayed impaired working and spatial memory when compared with nontransgenic control mice. By contrast, 3xTgAD mice maintained on the PRC regimen for 18–19 weeks did not perform significantly worse than WT mice. Moreover, it is worth noting that all the behavioral tests were performed during the normal diet refeeding period, ruling out that the effects are temporary and lasting only during the protein restriction. Interestingly, two important features of AD pathology, A $\beta$  accumulation and microglia activation, were not modified in the hippocampus of protein restricted 3xTg-AD mice. On the other hand, we found that 3xTg-AD subjected to PRC regimen exhibited reduced phosphorylated tau levels compared with 3xTg-AD mice fed with normal diet. Evidence indicates a strong association between phosphorylated tau levels and cognitive deficits in human subjects afflicted by AD or mild cognitive impairment (MCI) (de Leon *et al.*, 2006). Our results support a role for reduced tau phosphorylation in alleviating memory impairment as indicated by studies conducted on AD models (Roberson *et al.*, 2007).

The beneficial effect of reduced tau phosphorylation independently of A $\beta$  deposition may be explained by the fact that A $\beta$  pathology precedes tau pathology in this AD model (Oddo *et al.*, 2003). In fact, whereas A $\beta$  deposition is present by 6 months of age in the hippocampus of 3xTg-AD mice, it is not until approximately 12 months that AT8 immunoreactivity for phosphorylated tau is readily detectable (Oddo *et al.*, 2003). Thus, levels of A $\beta$  in 3xTg-AD brains may not have been influenced by the PRC intervention, as also reported in previous studies on CR (Patel *et al.*, 2005; Wang *et al.*, 2005; Halagappa *et al.*, 2007; Mouton *et al.*, 2009) because of the advanced stage of A $\beta$  pathology at the beginning of the treatment.

In 3xTg-AD brains, extraneuronal A $\beta$  deposition also precedes microglia activation and plays a major role in the onset of inflammation (Kitazawa *et al.*, 2005). Therefore, the failure to detect an effect of protein restriction on microglia activation, as observed in previous studies on CR and brain aging (Wong *et al.*, 2005), may be due to the late onset of the dietary intervention.

The protein restriction regimen led to a modulation of circulating levels of IGF-1 and its binding proteins. The resulting reduction in IGF-1 signaling may be responsible, in part, for the improved outcome in the AD mice.

Recently, we have shown a reduced incidence of cancer and diabetes in GHR- and IGF-1-deficient subjects (Guevara-Aguirre *et al.*, 2011). The protective effect of low GH/IGF-1 signaling against age-related diseases observed in GHRD human subject is consistent with results from the GHR/IGF-1-deficient dwarf mice and the Tor/Sch9-deficient yeast (Brown-Borg *et al.*, 1996; Coschigano *et al.*, 2000; Fabrizio *et al.*, 2001; Fontana *et al.*, 2010). Although the known population of GHRDs is small (less than 400 around the

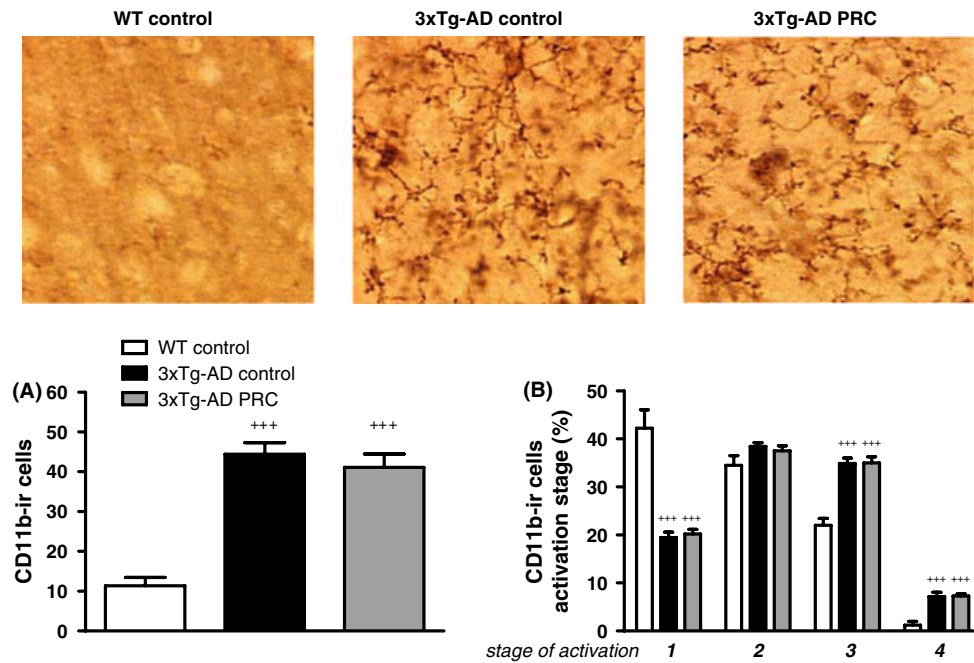


**Fig. 6** PRC regimen does not modulate total number nor activation stages of CD11b-ir cells in 3xTg-AD mice hippocampus. Representative images showing CD11b-immunoreactive (CD11b-ir) microglia in hippocampus sections of 12.5–13.5-month-old WT control, 3xTg-AD control and 3xTg-AD PRC mice are shown. Quantification of total number of CD11b-ir cells in the described experimental groups is shown in A. Percentage of different microglia activation stages (1–4) is represented in B (for all figures:  $+++P < 0.001$  compared with WT, 5–10 samples per group).

world) and few of them have reached ages above 80, no cases of AD have yet been reported in GHRDs, raising the possibility that their nervous system may also be protected from aging and dementia and underlining the need for additional studies in these subjects. Thus, interventions that down-regulate GHR/IGF-1 signaling such as protein restriction cycles should be tested for their potential to protect against aging and age-related diseases.

On the other hand, IGF-1 is critical for normal nervous system maintenance and is involved in major aspects of CNS, such as neuronal development and plasticity. Local IGF-1 availability in the brain can play a neuroprotective role in AD by increasing neurogenesis and neuronal survival and modulating brain A $\beta$  clearance (Carro *et al.*, 2002).

Our serum IGF-1 measurement showed significantly higher levels of this circulating hormone in 3xTg-AD mice compared with those in the WT group. Increased circulating IGF-1 has also been observed in AD patients (Vardy *et al.*, 2007) and may be caused by an attempt to overcome a state of resistance to IGF-1 signaling characterized by the loss of sensitivity to the hormone's action (Carro & Torres-Aleman, 2004). Recently, Arnold and co-workers provided direct demonstration that AD brain is IGF-1 resistant and showed that activated forms of molecules downstream the insulin/IGF-1 signaling are significantly elevated in AD patients brain (Talbot *et al.*, 2012).

Although we did not analyse brain IGF-1 signaling in this study, we speculate that the chronic systemic reduction in IGF-1 levels induced by the PRC regimen may increase IGF-1 sensitivity in 3xTg-AD brain leading to improved cognitive function and reduced tau

pathology. In agreement with our results, organotypic slices from hippocampi of adult Ames dwarf mice, characterized by increased IGF-1 protein levels in the hippocampus and circulating IGF-1 deficiency, are resistant to A $\beta$ -induced tau hyperphosphorylation (Schrag *et al.*, 2008). In addition, aging Ames and GHR-KO mice show better memory performance compared with age-matched WT littermates (Kinney *et al.*, 2001; Sharma *et al.*, 2010) and Ames mice exhibit increased neurogenesis following hippocampal insults (Sharma *et al.*, 2012), raising the possibility that reduction of circulating IGF-1 together with a higher level of this growth factor in the brain may provide additional protection and promote cognitive function via neuronal proliferation.

In conclusion, the results presented here show that PRCs are able to alleviate AD-like symptoms in 3xTg-AD mice possibly by modulating tau phosphorylation. Notably, this dietary intervention is not coupled to CR and does not cause apparent side effects in 3xTg-AD mice. These findings, combined with the fact that PRCs were effective on mice already showing significant AD-like symptoms, raise the possibility that PRCs could be clinically useful for long-term treatment of patients affected by AD. Treatment conditions applicable to patients should be established by determining the length of time required to achieve changes in IGF-1 and IGFBP-1 in humans similar to those by 1 week protein restriction in mice. Cycles of 1 week on normal diet and 1 week on a protein restricted diet supplemented with nonessential amino acids similar to those used here should be tested in clinical trials. In the future, more studies are needed to further investigate the safety of this promising treatment and to elucidate its mechanism of action.

## Experimental procedures

### Diet composition

The following experimental diets have been used:

- Normal diet (Harlan Teklad LM-485, Indianapolis, IN, USA).
- Protein Restriction (PR) Diet (diet lacking 9 AA: Isoleucine, Leucine, Lysine, Methionine, Phenylalanine, Threonine, Tryptophan, Valine, Arginine) (Teklad, Indianapolis, IN, USA).

Differently from the normal diet, PR diet does not contain proteins and the nitrogen sources are represented only by free AA. The two diets are similar in nitrogen content, thus similar in caloric density (Table 1). To maintain equivalent nitrogen content in normal and PR diets, we balanced the lack of designated AA by increasing the quantity of the remaining ones (Table 2).

Essential AA cannot be synthesized *de novo* by mammals and therefore must be supplied through the diet. Long-term essential AA depletion can cause severe health problems and eventually lead to death. Regimen of alternating normal and PR diets was chosen to overcome chronic depletion of essential AA. The following dietary regimens were used (Fig. 1A):

- Control (normal diet).
- Protein Restriction Cycle (PRC) (7 days of PR diet followed by 7 days of normal diet refeeding).

### Mice and experimental design

3xTg-AD and corresponding wild-type (WT) (C57BL/6/129S) mice were used in this study. 3xTg-AD mice overexpress three human genes harboring mutations linked to AD (presenelin-1, APP) and frontotemporal dementia (tau), that result in the development of both Aβ plaques, hyperphosphorylated tau tangles as well as the age-dependent Alzheimer-like cognitive impairment (Oddo *et al.*, 2003). Colonies of the described mice were bred and maintained at the University of Southern California in accordance with National Institutes of Health guidelines on use of laboratory animals and an approved protocol by the University of Southern California (Los Angeles, CA) Institutional Animal Care and Use Committee. Male 3xTg-AD and WT mice were single caged to monitor the food intake before the beginning of the diet regimen. At the age of 8–9 months [at this age cognitive deficits, such as working memory impairment, are detectable in 3xTg-AD mice, SFig. 2A and (Rosario *et al.*, 2006)] 3xTg-AD and WT animals were divided into two groups (12–14 mice per group) and assigned to the dietary regimens described above.

Mice were randomly assigned to dietary groups based on body weight (mean body weight of 29.6 g for 3xTg-AD, 32.4 g for WT). The rodents were maintained on 12 h light/dark cycles and provided *ad libitum* access to water and the described diets. Food was refreshed according with dietary regimen every 2 to 3 days (day 0, 2, and 4 of 7 days diet cycle). The animals were subjected to the PRC regimen for 18–19 weeks.

During the different dietary regimes, body weights were measured weekly. Furthermore, mice weight and food intake were measured every day at the beginning of dietary treatment, on week 1 and 2, and at the end, on week 17 and 18. Mice subjected to the different diet regimens that failed to regain weight during the

**Table 1** Ingredients, macronutrients composition, and caloric density of Normal and PR diets

	Ingredients (g kg <sup>-1</sup> )		Macronutrients (g kg <sup>-1</sup> )	
	Normal diet	PR diet	Normal diet	PR diet
Corn starch	397.49	397.49	Carbohydrate	601 617
Maltodextrin	132	146	Nitrogen source	187 183
Sucrose	100	100	Fat	72 72
Soybean oil	70	72		
Cellulose	50	50		
Mineral	35	35		
Vitamin	10	10		
Choline bitartrate	2.5	2.5		
TBHQ	0.01	0.01		
				Caloric density (kcal g <sup>-1</sup> )
				3.76 3.77

TBHQ, Tert-butylhydroquinone.

**Table 2** AA composition of Normal and PR diets expressed as g AA kg<sup>-1</sup> food

	AA mixture (g kg <sup>-1</sup> )	
	Normal diet	PR diet
Ala	10.0	8.3
Arg	12.0	0.0
Asp	18.0	20.1
Cys	3.0	6.3
Glu	28.0	63.9
Gly	8.0	7.7
His	5.0	8.6
Ile	8.0	0.0
Leu	17.0	0.0
Lys	10.0	0.0
Met	4.0	0.0
Phe	9.0	0.0
Pro	14.0	32.3
Ser	13.0	17.9
Thr	8.0	0.0
Trp	3.0	0.0
Tyr	8.0	17.9
Val	9.0	0.0
Total	187.0	183.1

refeeding period or showed signs of discomfort were removed from the study (one 3xTg-AD mouse from Control group and one from PRC group were excluded).

Before the start of the treatment and every 4 weeks during the dietary regimen, the mice were tested with Y-maze (hippocampus-dependent working memory) and Elevated Plus Maze (anxiety detection). At the end of the dietary intervention, the animals were subjected to Object Recognition Test (short-term spatial memory). To minimize any possible abnormal behavior caused by difference in diet composition, the behavioral tests were performed during the normal diet refeeding period.

At the end of diet treatment, the mice were sacrificed under isoflurane anesthesia and blood and brains collected. Blood was

collected by tail-snip for glucose measurement and by heart puncture for protein analyses. All the serum obtained was kept at  $-80^{\circ}\text{C}$  until assayed. The brain was divided into two: one hemisphere was dissected, frozen, and stored at  $-80^{\circ}\text{C}$ , the other was immersion fixed in fresh 4% paraformaldehyde/0.1 M PBS for 48 h and then stored at  $4^{\circ}\text{C}$  in 0.1 M PBS/0.2% sodium azide.

### Glucose measurement

Glucose levels were measured with blood collected by tail-snip using a Precision Xtra blood glucose monitoring system (Abbott, Abbott Park, IL, USA).

### IGF-1, IGFBP-3, and IGFBP-1 measurement

Mouse serum IGF-1 and IGFBP-3 levels were measured by in-house mIGF-1 and mIGFBP-3 ELISAs as previously described (Hwang *et al.*, 2008). The IGF-1 assay has a sensitivity of  $0.1\text{ ng mL}^{-1}$  and no cross-reactivity with IGF-2. The intraassay and interassay coefficients of variations (CV) were  $< 10\%$  in the range from 1 to  $10\text{ ng mL}^{-1}$ . The mouse IGFBP-3 assay has a sensitivity of  $0.2\text{ ng mL}^{-1}$ . The CVs of intraassay and interassay were  $< 6\%$  and  $< 8\%$ , respectively, in the range of  $1\text{--}6\text{ ng mL}^{-1}$ . Mouse serum IGFBP-1 levels were measured by in-house ELISA assays using recombinant mouse proteins and antibodies from R&D Systems (MAB 1240 as capture antibody and BAF 1240 as detection antibody, R&D Systems, Minneapolis, MN, USA). The assay has a sensitivity of  $0.1\text{ ng mL}^{-1}$  and the CVs of in intra- and interassay were  $< 10\%$ , respectively.

### Behavioral tests

#### Y-maze

A total of 12–14 mice per group were tested for working memory using a Y-maze [arms 21 cm (long) by 4 cm (wide) with 40-cm walls]. The mice were tested before the dietary intervention, at the age of 8–9 months, and every month of treatment till the age of 12.5–13.5 months. The test started by placing the mouse in one of the arms of the maze. The mouse was allowed to explore freely the environment for 8 min and the total numbers of arm entries and arm choices were recorded. An arm choice was defined as both forepaws and hindpaws fully entering the arm. Spontaneous alternation behavior (SAB) score was calculated as the proportion of alternations (an arm choice differing from the previous two choices) to the total number of alternation opportunities (Rosario *et al.*, 2006; Carroll *et al.*, 2010).

#### Novel Object Recognition (NOR) Test

A total of 12–14 mice per group were tested for short-term spatial memory using the Novel Object Recognition (NOR) test. The mice were tested once at the end of dietary treatment at the age of 12.5–13.5 months. The maze consists in an opaque plastic box measuring 61 cm (length)  $\times$  36 cm (width)  $\times$  30 cm (height). The test is based on the protocol described by Gulinello and co-workers (Gulinello *et al.*, 2009). Briefly, on the first day of the test (habituation day), the mouse was placed into the box and allowed to explore the field for

5 min. Twenty-four hours later (test day), habituated mouse was placed again into the box at the presence of two identical, nontoxic objects and let to freely explore them for 5 min (trial 1). The time spent exploring the objects was recorded, considering exploration any physical contact with an object and/or approach with obvious orientation to it within 5 cm. At the end of trial 1, the animal was returned to the home cage. After 3 min, the mouse was returned to the testing field where one of the familiar objects was replaced by a novel object. The mouse was allowed to explore the arena for 5 min and time exploring the objects monitored again. Recognition index (RI) was calculated as time the animal spent exploring the novel object to the total time spent exploring both the objects.

#### Elevated Plus Maze (EPM)

A total of 12–14 mice per group were tested for anxiety using an Elevated Plus Maze (EPM). The mice were tested before the dietary intervention, at the age of 8–9 months, and every month of treatment until the age of 12.5–13.5 months. The EPM has the shape of a cross formed by two alternate open and two alternate closed arms extending from a central platform, each arm measuring 30 cm length, 5 cm width, and 15 cm height (Carroll *et al.*, 2010). The test is based on rodent exploratory behavior, balanced by natural rodent aversion against open space. The avoidance of elevated open arms is an indication of the intensity of anxiety. During the test the mouse was placed onto the center field and allowed to freely explore the maze for 5 min, and the time spent in the open arms, corresponding to lower anxiety levels, was measured.

### Immunohistochemistry

A total of 8–10 fixed hemibrains per group were sectioned ( $40\text{ }\mu\text{m}$ ) exhaustively in the horizontal plane using a vibratome Leica V1000S (Leica, Nussloch, Germany) and then processed for immunohistochemistry. Every seventh section (10 per brain) was immunostained with antibodies directed against A $\beta$  (71-5800 A $\beta$ , Zymed Laboratories, San Francisco, CA, USA), hyperphosphorylated tau (AT8, Pierce, Rockford, IL, USA) or CD11b (MCA711, Serotec, Kidlington, UK) using ABC Vector Elite and DAB kits (Vector Laboratories, Burlingame, CA, USA). For all the experiments, the immunoreactivity quantification was assessed by two observers blind to sample identity and the values were averaged.

#### A $\beta$

To enhance A $\beta$  immunoreactivity (IR), sections were rinsed for 5 min in 99% formic acid. A $\beta$  IR was calculated as load values. Briefly, selected fields of nonoverlapping immunolabeled sections of hippocampus (two fields for subiculum and three for CA1–*Cornu Ammonis* area 1) were captured and digitized using a video capture system coupled to a microscope. Using NIH Scion image 1.62C software, images were converted into binary/negative data and the positive pixels (equivalent to IR area) quantified (Carroll *et al.*, 2010). Also, A $\beta$  plaques were defined as extracellular A $\beta$ -immunoreactive deposits exhibiting a spherical shape and morphology distinct from intraneuronal A $\beta$  IR (Rosario *et al.*, 2006). For quantification combined hippocampal CA1 and subiculum regions from the

sections defined above were examined under light microscopy and the total number of extracellular plaques was counted. The area of each plaque was quantified using ImageJ software.

#### Tau

AT8-immunoreactive neurons were defined as cells showing strong AT8 immunolabeling over most of the cell surface. The positive cells were been counted within the combined hippocampal CA1 and subiculum regions (Carroll et al., 2010).

#### CD11b

CD11b-immunoreactive (ir) positive microglia cells were defined as cells covered by CD11b immunostaining over the cell body and processes. CD11b-ir cells were been counted in two adjacent nonoverlapping immunolabeled sections (five sections in total) of the combined hippocampal subiculum and CA1 regions. Moreover, the stage of cells activation was identified by their morphology. Briefly, we defined four stages of microglia activation (Zhang et al., 2011):

- Stage 1: Resting microglia. Rod-shaped soma with many long thin ramified processes.
- Stage 2: Activated ramified microglia. Elongated cell body, the processes are thicker.
- Stage 3: Amoeboid microglia showing a marked cellular hypertrophy and short and thick processes.
- Stage 4: Phagocytic cells. Round cells, processes are not detectable.

CD11b-ir cells in the different activation stages were counted and plotted as percentage of the total ir cell number.

#### Statistical analysis

Body weight and calories intake changes over the time were analyzed by repeated measures ANOVA followed by Newman–Keuls test. Other data were analyzed by One-way ANOVA followed by between-group comparisons using the Fisher's least significant difference test. T-test was used when suitable. All the data represent mean  $\pm$  SEM.

#### Acknowledgments

We are thankful to Sebastian Brandhorst, Changhan Lee, and Sangeeta Bardhan Cook for the help in mice food intake monitoring. We thank Inyoung Choi for the help in mice tissue collecting. Finally, we are grateful to Professor Christian Pike for the use of the vibratome. This study was supported, in part, by a NIH Grant P01 AG034906 to VL.

#### Author contributions

The experiments were designed by EP, MW, and VDL and carried out by EP, TM, FM, LZ, and JW. The manuscript was prepared by EP and VDL with PC and LF assistance.

#### References

- Bokov AF, Garg N, Ikeno Y, Thakur S, Musi N, DeFronzo RA, Zhang N, Erickson RC, Gelfond J, Hubbard GB, Adamo ML, Richardson A (2011) Does reduced IGF-1R signaling in *Igf1r*<sup>+/-</sup> mice alter aging? *PLoS ONE* **6**, e26891.

- Brown-Borg HM, Borg KE, Meliska CJ, Bartke A (1996) Dwarf mice and the ageing process. *Nature* **384**, 33.
- Carro E, Torres-Aleman I (2004) Insulin-like growth factor I and Alzheimer's disease: therapeutic prospects? *Expert Rev. Neurother.* **4**, 79–86.
- Carro E, Nunez A, Busiguina S, Torres-Aleman I (2000) Circulating insulin-like growth factor I mediates effects of exercise on the brain. *J. Neurosci.* **20**, 2926–2933.
- Carro E, Trejo JL, Gomez-Isla T, LeRoith D, Torres-Aleman I (2002) Serum insulin-like growth factor I regulates brain amyloid-beta levels. *Nat. Med.* **8**, 1390–1397.
- Carroll JC, Rosario ER, Villamagna A, Pike CJ (2010) Continuous and cyclic progesterone differentially interact with estradiol in the regulation of Alzheimer-like pathology in female 3xTransgenic-Alzheimer's disease mice. *Endocrinology* **151**, 2713–2722.
- Cohen E, Paulsson JF, Blinder P, Burstyn-Cohen T, Du D, Estepa G, Adame A, Pham HM, Holzenberger M, Kelly JW, Maslah E, Dillin A (2009) Reduced IGF-1 signaling delays age-associated proteotoxicity in mice. *Cell* **139**, 1157–1169.
- Coschigano KT, Clemmons D, Bellush LL, Kopchick JJ (2000) Assessment of growth parameters and life span of GHR/BP gene-disrupted mice. *Endocrinology* **141**, 2608–2613.
- Fabrizio P, Pozza F, Pletcher SD, Gendron CM, Longo VD (2001) Regulation of longevity and stress resistance by Sch9 in yeast. *Science* **292**, 288–290.
- Fontana L, Weiss EP, Villareal DT, Klein S, Holloszy JO (2008) Long-term effects of calorie or protein restriction on serum IGF-1 and IGFBP-3 concentration in humans. *Ageing Cell* **7**, 681–687.
- Fontana L, Partridge L, Longo VD (2010) Extending healthy life span—from yeast to humans. *Science* **328**, 321–326.
- Fontan-Lozano A, Lopez-Lluch G, Delgado-Garcia JM, Navas P, Carrion AM (2008) Molecular bases of caloric restriction regulation of neuronal synaptic plasticity. *Mol. Neurobiol.* **38**, 167–177.
- Gietzen DW, Hao S, Anthony TG (2007) Mechanisms of food intake repression in indispensable amino acid deficiency. *Annu. Rev. Nutr.* **27**, 63–78.
- Goedert M, Jakes R, Vanmechelen E (1995) Monoclonal antibody AT8 recognises tau protein phosphorylated at both serine 202 and threonine 205. *Neurosci. Lett.* **189**, 167–169.
- Guevara-Aguirre J, Balasubramanian P, Guevara-Aguirre M, Wei M, Madia F, Cheng CW, Hwang D, Martin-Montalvo A, Saavedra J, Ingles S, de Cabo R, Cohen P, Longo VD (2011) Growth hormone receptor deficiency is associated with a major reduction in pro-aging signaling, cancer, and diabetes in humans. *Sci. Transl. Med.* **3**, 70ra13.
- Gulinello M, Gertner M, Mendoza G, Schoenfeld BP, Oddo S, LaFerla F, Choi CH, McBride SM, Faber DS (2009) Validation of a 2-day water maze protocol in mice. *Behav. Brain Res.* **196**, 220–227.
- Halagappa VK, Guo Z, Pearson M, Matsuoka Y, Cutler RG, Laferla FM, Mattson MP (2007) Intermittent fasting and caloric restriction ameliorate age-related behavioral deficits in the triple-transgenic mouse model of Alzheimer's disease. *Neurobiol. Dis.* **26**, 212–220.
- Hwang DL, Lee PD, Cohen P (2008) Quantitative ontogeny of murine insulin-like growth factor (IGF)-I, IGF-binding protein-3 and the IGF-related acid-labile subunit. *Growth Horm. IGF Res.* **18**, 65–74.
- Ikeno Y, Hubbard GB, Lee S, Cortez LA, Lew CM, Webb CR, Berryman DE, List EO, Kopchick JJ, Bartke A (2009) Reduced incidence and delayed occurrence of fatal neoplastic diseases in growth hormone receptor/binding protein knockout mice. *J. Gerontol. A Biol. Sci. Med. Sci.* **64**, 522–529.
- Jones JL, Clemmons DR (1995) Insulin-like growth factors and their binding proteins: biological actions. *Endocr. Rev.* **16**, 3–34.
- Kenyon C (2005) The plasticity of aging: insights from long-lived mutants. *Cell* **120**, 449–460.
- Ketelslegers JM, Maiter D, Maes M, Underwood LE, Thissen JP (1995) Nutritional regulation of insulin-like growth factor-I. *Metabolism* **44**, 50–57.
- Kinney BA, Coschigano KT, Kopchick JJ, Steger RW, Bartke A (2001) Evidence that age-induced decline in memory retention is delayed in growth hormone resistant GH-R-KO (Laron) mice. *Physiol. Behav.* **72**, 653–660.
- Kitazawa M, Oddo S, Yamasaki TR, Green KN, LaFerla FM (2005) Lipopolysaccharide-induced inflammation exacerbates tau pathology by a cyclin-dependent kinase 5-mediated pathway in a transgenic model of Alzheimer's disease. *J. Neurosci.* **25**, 8843–8853.
- Lee C, Longo VD (2011) Fasting vs dietary restriction in cellular protection and cancer treatment: from model organisms to patients. *Oncogene* **30**, 3305–3316.
- de Leon MJ, DeSanti S, Zinkowski R, Mehta PD, Pratico D, Segal S, Rusinek H, Li J, Tsui W, Saint Louis LA, Clark CM, Tarshish C, Li Y, Lair L, Javier E, Rich K, Lesbre P, Mosconi L, Reisberg B, Sadowski M, DeBernadis JF, Kerkman DJ, Hampel H, Wahlund LO, Davies P (2006) Longitudinal CSF and MRI biomarkers improve the diagnosis of mild cognitive impairment. *Neurobiol. Aging* **27**, 394–401.

- Longo VD, Finch CE (2003) Evolutionary medicine: from dwarf model systems to healthy centenarians? *Science* **299**, 1342–1346.
- Luchsinger JA, Tang MX, Shea S, Mayeux R (2002) Caloric intake and the risk of Alzheimer disease. *Arch. Neurol.* **59**, 1258–1263.
- Martin B, Mattson MP, Maudsley S (2006) Caloric restriction and intermittent fasting: two potential diets for successful brain aging. *Ageing Res. Rev.* **5**, 332–353.
- Masternak MM, Panici JA, Bonkowski MS, Hughes LF, Bartke A (2009) Insulin sensitivity as a key mediator of growth hormone actions on longevity. *J. Gerontol. A Biol. Sci. Med. Sci.* **64**, 516–521.
- Mattson MP (2005) Energy intake, meal frequency, and health: a neurobiological perspective. *Annu. Rev. Nutr.* **25**, 237–260.
- Mouton PR, Chachich ME, Quigley C, Spangler E, Ingram DK (2009) Caloric restriction attenuates amyloid deposition in middle-aged dtg APP/PS1 mice. *Neurosci. Lett.* **464**, 184–187.
- Oddo S, Caccamo A, Kitazawa M, Tseng BP, LaFerla FM (2003) Amyloid deposition precedes tangle formation in a triple transgenic model of Alzheimer's disease. *Neurobiol. Aging* **24**, 1063–1070.
- Parrella E, Longo VD (2010) Insulin/IGF-I and related signaling pathways regulate aging in nondividing cells: from yeast to the mammalian brain. *Sci. World J.* **10**, 161–177.
- Patel NV, Gordon MN, Connor KE, Good RA, Engelman RW, Mason J, Morgan DG, Morgan TE, Finch CE (2005) Caloric restriction attenuates A $\beta$ -deposition in Alzheimer transgenic models. *Neurobiol. Aging* **26**, 995–1000.
- Roberson ED, Searce-Levie K, Palop JJ, Yan F, Cheng IH, Wu T, Gerstein H, Yu GQ, Mucke L (2007) Reducing endogenous tau ameliorates amyloid  $\beta$ -induced deficits in an Alzheimer's disease mouse model. *Science* **316**, 750–754.
- Rosario ER, Carroll JC, Oddo S, LaFerla FM, Pike CJ (2006) Androgens regulate the development of neuropathology in a triple transgenic mouse model of Alzheimer's disease. *J. Neurosci.* **26**, 13384–13389.
- Schrag M, Sharma S, Brown-Borg H, Ghribi O (2008) Hippocampus of Ames dwarf mice is resistant to beta-amyloid-induced tau hyperphosphorylation and changes in apoptosis-regulatory protein levels. *Hippocampus* **18**, 239–244.
- Sharma S, Haselton J, Rakoczy S, Branshaw S, Brown-Borg HM (2010) Spatial memory is enhanced in long-living Ames dwarf mice and maintained following kainic acid induced neurodegeneration. *Mech. Ageing Dev.* **131**, 422–435.
- Sharma S, Darland D, Lei S, Rakoczy S, Brown-Borg HM (2012) NMDA and kainate receptor expression, long-term potentiation, and neurogenesis in the hippocampus of long-lived Ames dwarf mice. *Age (Dordr)* **34**, 609–620.
- Sonntag WE, Lynch CD, Cefalu WT, Ingram RL, Bennett SA, Thornton PL, Khan AS (1999) Pleiotropic effects of growth hormone and insulin-like growth factor (IGF)-1 on biological aging: inferences from moderate caloric-restricted animals. *J. Gerontol. A Biol. Sci. Med. Sci.* **54**, B521–B538.
- Suh Y, Atzmon G, Cho MO, Hwang D, Liu B, Leahy DJ, Barzilai N, Cohen P (2008) Functionally significant insulin-like growth factor I receptor mutations in centenarians. *Proc. Natl. Acad. Sci. U S A* **105**, 3438–3442.
- Talbot K, Wang HY, Kazi H, Han LY, Bakshi KP, Stucky A, Fuino RL, Kawaguchi KR, Samoyedny AJ, Wilson RS, Arvanitakis Z, Schneider JA, Wolf BA, Bennett DA, Trojanowski JQ, Arnold SE (2012) Demonstrated brain insulin resistance in Alzheimer's disease patients is associated with IGF-1 resistance, IRS-1 dysregulation, and cognitive decline. *J. Clin. Invest.* **122**, 1316–1338.
- Thissen JP, Ketelslegers JM, Underwood LE (1994) Nutritional regulation of the insulin-like growth factors. *Endocr. Rev.* **15**, 80–101.
- Vardy ER, Rice PJ, Bowie PC, Holmes JD, Grant PJ, Hooper NM (2007) Increased circulating insulin-like growth factor-1 in late-onset Alzheimer's disease. *J. Alzheimers Dis.* **12**, 285–290.
- Wang J, Ho L, Qin W, Rocher AB, Seror I, Humala N, Maniar K, Dolios G, Wang R, Hof PR, Pasinetti GM (2005) Caloric restriction attenuates beta-amyloid neuropathology in a mouse model of Alzheimer's disease. *FASEB J.* **19**, 659–661.
- Wong AM, Patel NV, Patel NK, Wei M, Morgan TE, de Beer MC, de Villiers WJ, Finch CE (2005) Macrosialin increases during normal brain aging are attenuated by caloric restriction. *Neurosci. Lett.* **390**, 76–80.
- Wu P, Shen Q, Dong S, Xu Z, Tsien JZ, Hu Y (2008) Calorie restriction ameliorates neurodegenerative phenotypes in forebrain-specific presenilin-1 and presenilin-2 double knockout mice. *Neurobiol. Aging* **29**, 1502–1511.
- Yamamoto H, Murphy LJ (1995) Enzymatic conversion of IGF-I to des(1–3)IGF-I in rat serum and tissues: a further potential site of growth hormone regulation of IGF-I action. *J. Endocrinol.* **146**, 141–148.
- Young SN (1996) Behavioral effects of dietary neurotransmitter precursors: basic and clinical aspects. *Neurosci. Biobehav. Rev.* **20**, 313–323.
- Zhang S, Wang XJ, Tian LP, Pan J, Lu GQ, Zhang YJ, Ding JQ, Chen SD (2011) CD200-CD200R dysfunction exacerbates microglial activation and dopaminergic neurodegeneration in a rat model of Parkinson's disease. *J. Neuroinflammation* **8**, 154.

## Supporting Information

Additional Supporting Information may be found in the online version of this article at the publisher's web-site.

**Fig. S1** Food intake was measured and used to calculate calories intake. Calories intake normalized for grams of body weight was scored daily at the beginning (weeks 1 and 2, A) and at the end of the dietary treatment (weeks 17–18, B) and was expressed as percentage calculated for the first week (days 1–7, PR diet) or the second week (days 8–14, refeeding with normal diet) of diet cycle compared with control diets values scored during the same periods (\* $P < 0.05$ , \*\* $P < 0.01$ , \*\*\* $P < 0.001$ ).

**Fig. S2** (A) Shown is SAB (spontaneous alternation behavior), obtained testing the mice with Y-maze after 12 weeks of PRC regimen. 3xTg-AD groups performed worse than WT control group (\* $P < 0.05$ , 13–14 mice per group). (B) Shown is the time spent in open arms scored testing the mice with EPM at 8–9 months of age, before any dietary treatment. We did not detect significant difference in the scored parameter (13–14 mice per group).

**Fig. S3** After 18 weeks of diet intervention, the mice were tested on Y-maze and NOR tests. (A) Shown is the number of arm entries scored during the Y-maze task. We did not detect significant difference among WT and 3xTg-AD groups (13–14 mice per group). (B) On trial 1 of NOR test, the rodents were allowed to explore a box containing two identical objects (object A and object B) and the time spent exploring them was recorded. No significant difference was found in the time the animals dedicated to explore the different objects ( $t$ -test: time object A vs. time object B, 12–14 mice per group).